



## ORIGINAL ARTICLE

# Catalytic behavior of gallium-containing mesoporous silicas



K. Bachari <sup>a,\*</sup>, R.M. Guerroudj <sup>a</sup>, M. Lamouchi <sup>b</sup>

<sup>a</sup> Centre de recherche scientifique et technique en analyses physico-chimiques (C.R.AP.C) BP 248, Alger RP 16004, Algiers, Algeria

<sup>b</sup> Laboratoire de Catalyse et Environnement, EA 2598, MREI, Université du Littoral-Cote d'Opale, 145, Avenue Maurice Schumann, 59140 Dunkerque Cedex, France

Received 3 May 2012; accepted 29 July 2012

Available online 11 August 2012

## KEYWORDS

Tert-butylation;  
Anisole;  
Ga-mesoporous materials;  
4-Tert-butyl anisole

**Abstract** The vapor phase tert-butylation of anisole with tert-butanol reaction has been inspected over a series of Ga-FSM-16 with different Si/Ga ratios = 75, 35, 5 synthesized by intercalating kanemite using cetyltrimethylammonium bromide (CTMABr) and gallium nitrate. The resulting samples were characterized by means of inductively coupled plasma (ICP) technique, BET, BJH, XRD and a temperature-programmed-desorption (TPD) of pyridine. In addition, the influence of molar ratio, influence of temperature, weight hourly space velocity (WHSV) and time on stream on the selectivity of products was investigated and the results are discussed.

© 2012 Production and hosting by Elsevier B.V. on behalf of King Saud University. This is an open access article under the CC BY-NC-ND license (<http://creativecommons.org/licenses/by-nc-nd/3.0/>).

## 1. Introduction

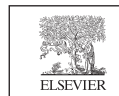
Folded Sheet Mesoporous material (FSM-16) was first synthesized by intercalation of a layered sodium silicate kanemite with long chain cetyltrimethylammonium (CTMA) ions at 343 K followed by adjustment of the pH of the suspension to 8.5 and then calcination of the resulting CTMA-kanemite complex at 823 K in air (Yanagisawa et al., 1990). FSM-16 materials, which are analogous to the most extensively studied MCM-41 (hexagonal, p6 mm) materials, have gained much attention because of their high surface areas and pore volumes (Inagaki et al., 1993; Kuroda, 1996; Sakamoto et al., 1998).

They possess a hexagonal array of channels with narrow pore size distributions. On the other hand, FSM-16 materials are formed via a folded sheet mechanism in which the condensation of the reactive silanol groups present on the adjacent silicate layers in CTMA kanemite complex leads to the formation of a hexagonal array of channels with uniform pore size (Inagaki et al., 1993). This mechanism is further substantiated by in situ energy dispersive X-ray diffraction (EDXRD) measurements (Chen et al., 1999). It is noteworthy that in comparison to MCM-41 materials, FSM-16 materials exhibit improved thermal stability, which is one of the key requirements for potential catalytic applications. This observed thermal stability can be attributed to their thicker pore walls. In fact, FSM-16 materials have widely been used as hosts to immobilize enzymes (Fujishima et al., 2001) and metal complexes (Yoshida et al., 1997; Inaki et al., 2000; Shouro et al., 2001; Fukuoka et al., 2001a). Photofunctional [Ru (bpy)<sub>3</sub>]Cl<sub>2</sub>/FSM-16 materials are currently under increased investigation for the high potential they offer in the photooxidation of benzene to phenol (Fukuoka et al., 2001b). FSM-16 materials are also known to be effective catalysts for reactions such as photometathesis of

\* Corresponding author. Tel./fax: +0021321247406.

E-mail address: bachari2000@yahoo.fr (K. Bachari).

Peer review under responsibility of King Saud University.



Production and hosting by Elsevier

propene (Bachari et al., 2011; Yamamoto et al., 1998) and Beckmann rearrangement of cyclohexanone oxime to  $\epsilon$ -caprolactum (Yamamoto et al., 1999). Recently, the preparations of Pt, Rh, Fe and Ga nanoparticles in FSM-16 have also been reported (Dapaah et al., 1999; Olah, 1973; Hentit et al., 2007; Tahir et al., 2008). The acidic properties of FSM-16 materials and their applications in acid-catalyzed reactions have been reported (Tahir et al., 2008; Benadji et al., 2010; Merabti et al., 2010). Fe-modified FSM-16 has also been reported to possess high Bronsted acidity (Du et al., 2006). On the other hand, Friedel–Crafts reactions comprise a very important class of reactions which are of common use in organic chemistry. These reactions are habitually catalyzed by Lewis acids in liquid phase and the substitution of liquid acids by solid acid catalysts is a challenging task (Olah, 1973; Hentit et al., 2007; Tahir et al., 2008; Benadji et al., 2010; Merabti et al., 2010). In fact, the alkylation of anisole with tert-butanol (TBA) is a reaction of industrial importance as alkoxy benzenes are used as antioxidants, dye developers and stabilizers for fats, oils, plastic, rubber, etc. (Shouro et al., 2001). Only few reports are available in the literature. The alkylation of anisole using tert-butanol to yield 4-tert-butyl anisole was reported in the presence of  $ZrCl_4$  (Fukuoka et al., 2001a) and trifluoroacetic acid (Fukuoka et al., 2001b) and tert-butyl acetate was used as an alkylating agent in the presence of  $H_2SO_4$  (Bachari et al., 2010). Yadav et al. (2011) studied the same reaction using methyl-tert-butyl ether over solid acid catalysts and reported that DTP/K10 as more active. The same reaction was also reported over AIMCM-41 and  $H_3PW_{12}O_{40}$  supported on AIMCM-41 molecular sieves (Yamamoto et al., 1998; Yamamoto et al., 1999). However, the use of gallium mesoporous molecular sieves in this reaction is infrequent. In the present study we have reported the synthesis and characterization of gallium -incorporated FSM-16 mesoporous molecular sieves with different Si/Ga ratios = 75, 35, 5 and their application in the alkylation of anisole using tert-butanol reaction under vapor phase condition.

## 2. Experimental

### 2.1. Synthesis of the catalysts

Hydrothermal syntheses of mesoporous Ga-FSM-16 materials with different Si/Ga ratios were carried out using the typical procedure: kanemite (2.2 g) was added into a beaker containing a mixture of CTMABr (0.79 g) and 38.0 ml of deionized water and stirred for 45 min. And then gallium nitrate ( $Ga(NO_3)_3$ ) (0.23 g) was added dropwise into the above mixture. This mixture was stirred for another 45 min. The resultant mixture was transferred into a stainless-steel autoclave (60 ml) and heated to 373 K for 24 h under static conditions. The resultant product was filtered, washed thoroughly with deionized water, dried at 333 K and then calcined at 973 K in air for 12 h.

### 2.2. Characterization techniques

The X-ray diffraction (XRD) patterns of samples were recorded with a powder XRD instrument (Rigaku D/max 2500PC) with Cu  $K\alpha$  radiation ( $\lambda = 0.15418$  nm). It was operated at 40 kV and 50 mA. The experimental conditions corre-

spond to a step width of  $0.02^\circ$  and the scan speed of 10/min. The diffraction patterns were recorded in the  $2\theta$  range of  $1-10^\circ$ . Specific surface area and pore size were measured by using a NOVA2000e analytical system made by Quantachrome Corporation (USA). The specific surface area was calculated by Brunauer-Emmett-Teller (BET) method. Pore size distribution and pore volume were calculated by Barrett-Joyner-Halenda (BJH) method. The gallium content in the samples was determined by the inductively coupled plasma (ICP) technique (Vista-MAX, Varian). The density and strength of the acid sites of the different Ga-FSM-16 samples were determined by the temperature-programed desorption (TPD) of pyridine. About 100 mg of the materials were evacuated for 3 h at 523 K under vacuum ( $P < 10^{-5}$  kPa). Thereafter, the samples were cooled to room temperature under dry nitrogen followed by exposure to a stream of pyridine in nitrogen for 30 min. Subsequently, the physisorbed pyridine was removed by heating the sample to 393 K for 2 h in a nitrogen flow. The temperature-programed desorption (TPD) of pyridine was performed by heating the sample in nitrogen flow (50 ml/min) from 393 to 873 K with a rate of 10 K/min using a high-resolution thermogravimetric analyzer coupled with a mass spectrometer (SETARAM setsys 16MS). The observed weight loss was used to quantify the number of acid sites assuming that each mole of pyridine corresponds to one mole of protons.

### 2.3. Catalytic testing

Tertiary butylation of anisole was carried out in a fixed bed-vertical flow type reactor made up of Borosil glass tube 40 cm in length and 2 cm in internal diameter. The catalyst (0.5 g), diluted with a fourfold amount of porcelain beads of equal size, was loaded at the center of the reactor and supported on either side with a thin layer of quartz wool. The reactor was heated to the requisite temperature with the help of a tubular furnace controlled by a digital temperature controller cum indicator. The catalyst was activated at 773 K for 5 h in a flow of dry air before the reaction was conducted. Reactants were introduced into the reactor using a syringe pump. The bottom of the reactor was connected to a coiled

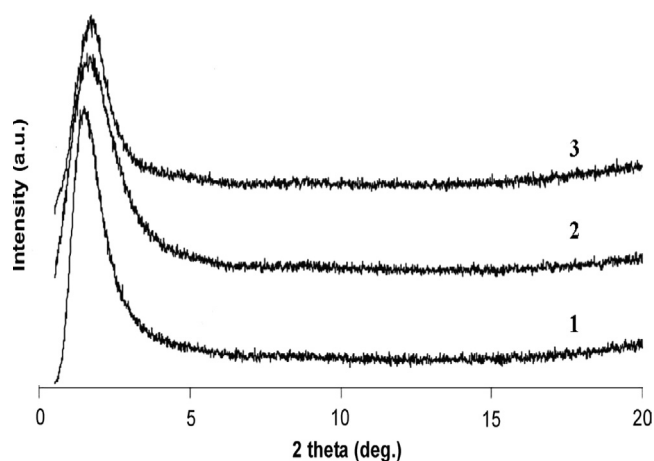


**Figure 1** XRD patterns of Ga-FSM-16 materials in the domain of  $1-10^\circ$  ( $2\theta$ ): (a) Ga-FSM-16 (75), (b) Ga-FSM-16 (35), (c) Ga-FSM-16 (5).

condenser and a receiver to collect the products. The products were chilled, collected, and analyzed by GC (Perkin Elmer, Elite 5MS capillary column) and products were confirmed with GC-MS (HP-5973) analysis.

### 3. Results

#### 3.1. Characterization of the samples

The small angle X-ray diffraction patterns of Ga-FSM-16 (Si/Ga = 75, 35, 5) are shown in Fig. 1. The unit-cell parameter ( $a_o$ ) values calculated from the peak with (hkl) = (100) using the equation  $a_o = 2d_{100}/\sqrt{3}$  are summarized in Table 1. The Ga-FSM-16 (75) sample gives a very strong (100) peak corresponding to the ordered hexagonal mesoporous structure. However, when the gallium content ratio increased from 35 to 5, the intensities of the long range ordered peaks were gradually reduced. However, compared with the pattern of the typical FSM-16 mesoporous molecular sieve (Yanagisawa et al., 1990), it can be noted that the  $d_{100}$  spacing in Ga-FSM-16 samples is significantly larger than FSM-16 that demonstrates the incorporation of gallium in the FSM-16 structure. At the same time, no diffraction lines corresponding to bulk gallium species could be observed in the 10–80° (2 $\theta$ ). The gallium content in Ga-FSM-16 is increased with gallium content in the synthesis gel (Table 1). The specific surface areas and pore size distributions and pore volumes calculated by BET and BJH methods are summarized in Table 1. From this table, we can conclude that the specific surface area and pore volume of the resulting samples gradually decreased as the gallium content increased, and the pore size is in the range of 2.2–2.7 nm. Moreover, the acid site distribution and acid amounts of Ga-FSM-16 were determined using temperature-programed-desorption (TPD) of pyridine and the data are collected in Table 2. Weak (423 and 633 K), moderate (633–743 K) and strong (> 743 K) acid sites are found in all samples. The weak acid sites are attributed to surface hydroxyl groups and the medium and the strong acid sites originate probably from the incorporation of gallium atoms into the FSM-16 walls. It is interesting to note that the number of weak acid sites decreases with decreasing Si/Ga ratio. However, the amount of medium and strong acid sites decreases with increasing Si/Ga ratio. It should be noted that the total number of acid sites (medium and strong acid sites) of Ga-FSM-16 (5) is higher than that of Ga-FSM-16 (35) and Ga-FSM-16 (75).

#### 3.2. Catalytic activity

##### 3.2.1. Catalytic performances of Gallium-FSM-16 catalysts in the vapor phase tert-butylation of anisole with tert-butanol

The vapor phase tert-butylation of anisole over Ga-FSM-16 catalysts was carried out at 423, 473, and 523 K with molar ratio

ANS/TBA = 3 and WHSV of 3.5 h<sup>-1</sup>. The results are presented in Table 3 and Fig. 2. The major products were 2-tert-butyl anisole (2-TBA), 4-tert-butyl anisole (4-TBA) and 2,4-ditert-butyl anisole (2,4-DTBA). In addition 3-tert-butyl anisole (3-TBA), dimerized and oligomerized butenes were also obtained. The conversion increases from 423 to 473 K, but decreases after that for all the catalysts. The decrease in conversion is due to oligomerization of butenes that block the active sites of coke. Although the same trend in conversion is observed over all the catalysts, the activity of the catalyst followed the order Ga-FSM-16 (5) > Ga-FSM-16 (35) > Ga-FSM-16 (75). Therefore it is suggested that the density of acid sites on the catalyst surface is an important factor for tert-butylation. So far another factor to be considered is hydrophobic and hydrophilic properties of the catalysts (Du et al., 2006; Llewellyn et al., 1995) Since Ga-FSM-16 with high Si/Ga ratio is more hydrophobic than those with less Si/Ga ratios, the former catalysts can exhibit high activity with reactants, which are hydrophobic. Hence in reaction with Ga-FSM-16, acid strength, hydrophilic and hydrophobic properties are also important in addition to density of acid sites in accounting for the activity of the catalyst. The selectivity to 4-TBA increases with increase in temperature over all the catalysts. The Ga-FSM-16 (5) gives higher selectivity than other catalysts. The selectivity to 2-TBA decreases with increase in temperature, The selectivity to 2,4-DTBA displays similar tendency as that of 2-TBA supporting again the steric obstacle for substitution at the ortho position with respect to o-methyl grouping of 4-TBA. The selectivity to 2,4-DTBA also follows similar tendency for Ga-FSM-16 with Si/Ga = 35, 75 as that of Ga-FSM-16 (5). From this study it is concluded that the best temperature is found to be 473 K as it provides high conversion and selectivity in comparison to higher temperature.

#### 3.3. Effect of time on stream

The effect of time on stream and the activity of catalyst Ga-FSM-16 (5) was studied at 473 K with ANS/TBA molar ratio = 3 and WHSV 3.5 h<sup>-1</sup>. The results are illustrated in Fig. 3. The conversion of anisole decreases with increase in time on stream. It is due to coke formation. The catalyst appeared slightly black after 5 h of time on stream. The selectivity of 4-TBA increases is due to a gradual decrease in its conversion to 2,4-DTBA. As expected, the selectivity of 2,4-DTBA also decreases with increase in time on stream. The selectivity of 2-TBA explains high augmentation with time on stream. It is also due to gradual decrease in its conversion to 2,4-DTBA with increase in time on stream. The enhanced p-selectivity with time can be accounted in terms of coke induced p-selectivity. During time on stream, the coke formed over the catalysts blocks the pores and narrows the pore size, which favors para products.

**Table 1** Physicochemical properties of different Ga-FSM-16 samples.

Sample	Chemical analysis		$S_{BET}$ (m <sup>2</sup> .g <sup>-1</sup> )	Pore volume (cm <sup>3</sup> .g <sup>-1</sup> )	Pore diameter (nm)
	Si/Ga (gel)	Si/Ga			
Ga-FSM-16	5	5.6	653	0.63	2.7
Ga-FSM-16	35	34.4	788	0.84	2.5
Ga-FSM-16	75	77.2	989	0.93	2.2

**Table 2** Density and strength of acid sites of Ga-FSM-16 catalysts with different Si/Ga ratios (Si/Ga = 75, 35, 5).

Samples	Acid sites (mmol/g)			
	Weak (423–633 K)	Medium (633–743)	Strong (> 743)	Total (medium and strong acid sites)
Ga-FSM-16(5)	0.539	0.191	0.224	0.415
Ga-FSM-16(35)	0.601	0.123	0.179	0.302
Ga-FSM-16(75)	0.748	0.107	0.145	0.252

**Table 3** Tert- butylation of anisole over the Ga-FSM-16 catalysts at different reaction temperatures (Reaction conditions: molar ratio ANS/TBA = 3 and WHSV of 3.5 h<sup>-1</sup>).

Catalysts	Temperature(K)	Conversion (%)	Selectivity (%)			
			2-TBA	4-TBA	2,4-DTBA	Others
Ga-FSM-16(75)	423	65.6	10.7	53.9	16.6	18.8
	473	70.3	9.8	58.6	15.7	15.9
	523	55.2	8.2	64.4	11.6	15.8
Ga-FSM-16 (35)	423	69.5	11.6	58.2	19.3	10.9
	473	75.3	10.4	61.6	17.6	10.4
	523	66.5	7.7	67.5	13.8	11.0
Ga-FSM-16(5)	423	74.5	13.2	57.4	23.8	5.6
	473	80.3	2.8	64.7	19.3	3.2
	523	72.5	9.6	69.3	15.7	5.4

TBA: Tert-butyl anisole; DTBA: Di-tert-butyl anisole.

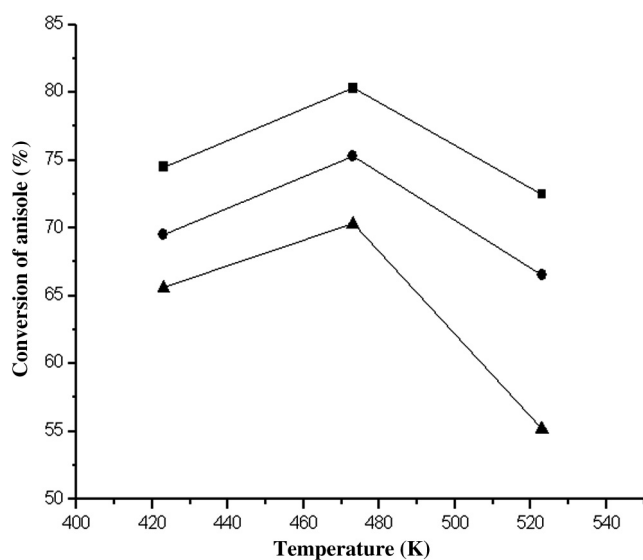


**Figure 2** Effect of reaction temperature on anisole conversion over different Ga-FSM-16 catalysts with different Si/Ga ratio (Reaction conditions: WHSV of 3.5 h<sup>-1</sup>, molar ratio ANS/TBA = 3 and, time on stream = 2).

#### 3.4. Effect of weight hourly space velocity (WHSV)

The effect of WHSV on the conversion of anisole of selectivity of the products was studied over Ga-FSM-16 (5) at 473 K, at 3.5 h<sup>-1</sup>, 4.5 h<sup>-1</sup> and 5.5 h<sup>-1</sup> with ANS/TBA molar ratio = 3 and is shown in Fig. 4. The conversion decreases with increase in WHSV. The selectivity 2-TBA is not much varied irrespective of the magnitude of increase in WHSV. The selectivity to 4-TBA increases with increase in WHSV due to reduced conversion of it to 2,4-DTBA. If the selectivity to 2-TBA, 4-TBA and 2, 4-

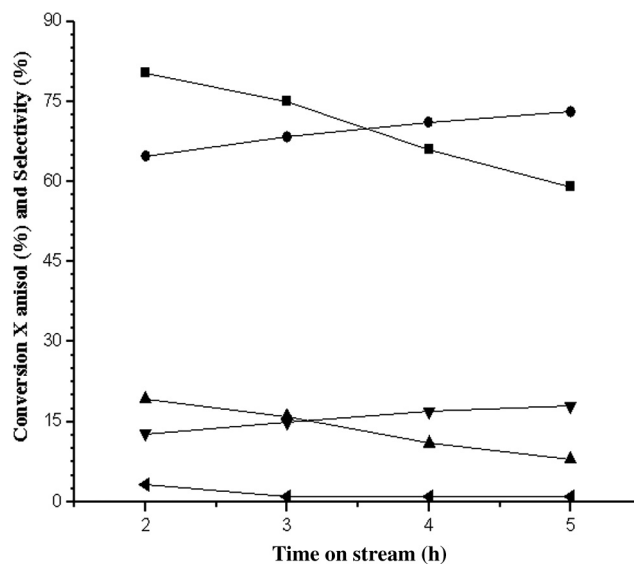


**Figure 3** Effect of time on stream on anisole conversion and product selectivity over Ga-FSM-16 (5) catalysts (Reaction conditions: T<sub>R</sub> = T<sub>R</sub> = 473 K, molar ratio ANS/TBA = 3, WHSV of 3.5 h<sup>-1</sup>).

DTBA is carefully analyzed, it will be evident that 2-TBA may not be making important contribution of 2,4-DTBA as the selectivity of it is very less.

#### 3.5. Effect of mole ratio ANS/TBA

The conversion of anisole was studied at 473 K over Ga-FSM-16 (5) with the different ANS/TBA molar ratio = 1, 2, 3 and WHSV 3.5 h<sup>-1</sup>. The results are illustrated in fig. 5. Since the

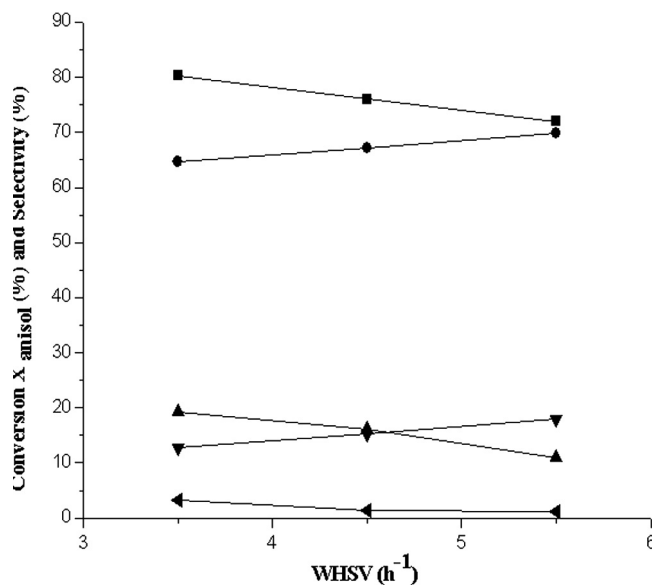


**Figure 4** Effect of a weight hourly space velocity (WHSV) on anisole conversion and product selectivity over Ga-FSM-16 (5) catalysts (Reaction conditions: molar ratio ANS/TBA = 3,  $T_R = 473$  K and, time on stream = 2).

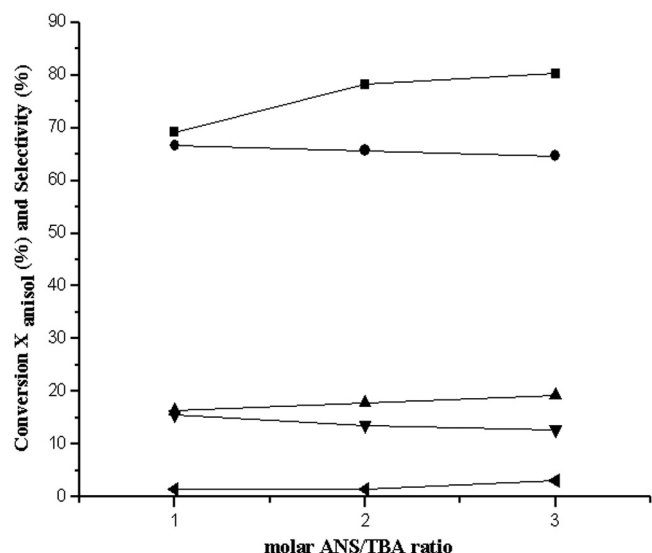


**Figure 5** Effect of molar ratio ANS/TBA on anisole conversion and product selectivity over Ga-FSM-16 (5) catalysts (Reaction conditions:  $T_R = 473$  K, WHSV of  $3.5 \text{ h}^{-1}$  and time on stream = 2).

reaction involves formation of tertbutyl cation on the catalyst surface the conversion increases with increase in the tertiary butyl alcohol in the feed. If the difference in conversion between 1, 2, and 3 is compared the former gives more increase in conversion than the latter. The selectivity to 2-TBA decreases but that of 2,4-DTBA increases with increase in the tert-butanol content in the feed. The 2-TBA might also be converted into 2,4-DTBA and the selectivity to 4-TBA decreases with the increase in the tert-butanol content in the feed.

#### 4. Conclusion

Gallium-FSM-16 with different Si/Ga ratios = 75, 35, 5 and with high specific surface area were successfully synthesized. After the synthesized sample was calcined at 813 K in air for 6 h, the template was effectively removed. The Si/Ga molar ratio is a key factor influencing the textural properties and structural regularity of Ga-FSM-16 mesoporous molecular sieves. The results of catalytic performance indicate that Ga-FSM-16 (10) was found to be more active than its relatives and the major products are found to be 4-tert-butyl anisole (4-TBA), 2-tert-butyl anisole (2-TBA) and 2,4 di-tert-butyl-anisole (2,4-DTBA).

#### References

- Bachari, K., Touileb, A., Saadi, A., Halliche, D., Cherifi, O., 2010. *J. Porous Mater.* 17, 573.
- Bachari, K., Guerroudj, R.M., Lamouchi, M., 2011. *React. Kinet. Mech. and Catal.* 102, 219.
- Benadji, S., Eloy, P., Leonard, A., Su, B.L., Bachari, K., Rabia, C., 2010. *Microp. and mesop. mater.* 130, 103.
- Chen, H., Matsumoto, A., Nishimiya, N., Tsutsumi, K., 1999. *Chem. Lett.* 993.
- Dapaah, J.K.A., Uemichi, Y., Ayame, A., Matsushashi, H., Sugioka, M., 1999. *Appl. Catal. A* 187, 107.
- Du, Y., Sun, Y., Di, Y., Zhao, L., Xiao, S., Liu F-S., 2006. *J. Porous Mater.* 13, 63.
- Fujishima, K., Fukuoka, A., Yamagishi, A., Inagaki, S., Fukushima, Y., Ichikawa, M., 2001. *J. Mol. Catal. A* 166, 211.
- Fukuoka, A., Higashimoto, N., Sakamoto, Y., Inagaki, S., Fukushima, Y., Ichikawa, M., 2001a. *Microporous Mesop. Mater.* 48, 171.
- Fukuoka, A., Higashimoto, N., Sakamoto, Y., Sasaki, M., Sugimoto, N., Inagaki, S., Fukushima, Y., Ichikawa, M., 2001b. *Catal. Today* 66, 23.
- Hentit, H., Bachari, K., Ouali, M.S., Womes, M., Benaichouba, B., Jumas, J.C., 2007. *J. Mol. Catal. A: Chem.* 275, 158.
- Inagaki, S., Fukushima, Y., Kuroda, K., 1993. *J. Chem. Soc. Chem. Commun.* 680.
- Inaki, Y., Yoshida, H., Kimura, K., Inagaki, S., Fukushima, Y., Hattori, T., 2000. *Phys. Chem. Chem. Phys.* 2, 5293.
- Kuroda, K., 1996. *J. Porous Mater.* 3, 107.
- Llewellyn, P.C., Schuth, F., Grillet, Y., Rouquerol, E., Unger, K.K., 1995. *Langmuir* 11, 574.
- Merabti, R., Bachari, K., Halliche, D., Rassoul, Z., Saadi, A., 2010. *React. Kinet., Mech. Catal.* 101, 195.
- Olah, G.A., 1973. *Friedel-Crafts Chemistry*. Wiley/ Interscience, New York.
- Sakamoto, Y., Inagaki, S., Ohsuna, T., Ohnishi, N., Fukushima, Y., Nozue, Y., Terasaki, O., 1998. *Microporous Mesop. Mater.* 589, 21.
- Shouro, D., Ohya, Y., Mishima, S., Nakajima, T., 2001. *Appl. Catal. A* 214, 59.
- Tahir, N., Abdellssadek, Z., Halliche, D., Saadi, A., Chebout, R., Cherifi, O., Bachari, K., 2008. *Surf. and Interface Analysis* 40, 254.
- Yamamoto, T., Tanaka, T., Funabiki, T., Yoshida, S., 1998. *J. Phys. Chem. B* 102, 5830.
- Yamamoto, T., Tanaka, T., Inagaki, S., Funabiki, T., Yoshida, S., 1999. *J. Phys. Chem. B* 103, 6450.
- Yanagisawa, T., Shimizu, T., Kuroda, K., Kato, C., 1990. *Bull. Chem. Soc. Jpn.* 63, 988.
- Yoshida, H., Kimura, K., Inaki, Y., Hattori, T., 1997. *Chem. Commun.* 129.